ASIAN JOURNAL OF PHARMACEUTICAL AND CLINICAL RESEARCH

INNOVARE ACADEMIC SCIENCES
Knowledge to Innovation

Vol 19, Issue 4, 2026

Online - 2455-3891
Print - 0974-2441

Research Article

THIOCOLCHICOSIDE-ASSISTED SILVER NANOPARTICLES FOR CONTROLLING WOUND PATHOGENS: *IN VITRO* ANTIBIOFILM ACTIVITY, PROTEIN AND DNA LEAKAGE AGAINST *PSEUDOMONAS AERUGINOSA* AND *ENTEROCOCCUS FAECALIS*

PARIVRAJ PRIYAM[1], RENU VAJJIRAVELU[2], ROHIT KUMAR SINGH[3], DEEPAK NALLASWAMY[3], SANTHOSHKUMAR JAYAKODI[2], RAJESHKUMAR SHANMUGAM[1]*

[1]Department of Anatomy, Saveetha Medical College and Hospital, Saveetha Institute of Medical and Technical Sciences, Chennai, Tamil Nadu, India. [2]Department of Biotechnology, Saveetha School of Engineering, Saveetha Institute of Medical and Technical Sciences, Chennai, Tamil Nadu, India. [3]Department of Prosthodontics, Saveetha Dental College and Hospitals, Saveetha Institute of Medical and Technical Sciences, Chennai, Tamil Nadu, India.

***Corresponding author: Rajeshkumar Shanmugam; Email: rajeshkumars.sdc@saveetha.com**

Received: 09 January 2025, Revised and Accepted: 02 March 2025

ABSTRACT

Objective: To synthesize silver nanoparticles (AgNPs) using *Gloriosa superba* extract and to functionalize with thiocolchicoside, and to evaluate their antibacterial, antibiofilm, protein leakage, cytoplasmic leakage, and time-dependent antimicrobial activities against Gram-positive and Gram-negative bacteria.

Methods: Aqueous extract of *G. superba* was mixed with silver nitrate ($AgNO_3$) to synthesize AgNPs, indicated by a color change from light to dark brown. Ultraviolet-visible (UV-vis) spectroscopy and transmission electron microscopy (TEM) were performed. Antibiofilm activity was measured by optical density (OD) against *Enterococcus faecalis* and *Pseudomonas* spp., while protein and cytoplasmic leakage assays assessed membrane damage. Antimicrobial activity and time-kill kinetics were tested against *E. faecalis*, *Escherichia coli*, *Pseudomonas* spp., and *Staphylococcus aureus* at 25–100 µg/mL.

Results: UV-vis spectra showed a peak at 250–270 nm, confirming nanoparticle formation. TEM images revealed spherical particles. TC-AgNCs reduced biofilm OD from 0.525±0.015 to 0.455±0.005 (*E. faecalis*) and 0.54±0.015 to 0.46±0.005 (*Pseudomonas* spp.) at 25–100 µg/mL. Protein leakage increased from 0.34±0.006 to 0.38±0.006, and cytoplasmic leakage from 0.28±0.01 to 0.38±0.01. Antimicrobial activity was observed at 100 µg/mL: *Pseudomonas* spp. (22.5±1.0), *E. faecalis* (18.5±0.9), *E. coli* (16.0±0.8), and *S. aureus* (18.0±0.9). Time-kill analysis showed a reduction in bacterial counts with increasing concentration and time.

Conclusion: TC-AgNCs synthesized using *G. superba* extract are stable, predominantly spherical, and exhibit strong dose- and time-dependent antibacterial and antibiofilm activity, with membrane-disruptive effects against both Gram-positive and Gram-negative bacteria.

Keywords: Antibiofilm activity, Protein and DNA leakage, *Pseudomonas aeruginosa*, Thiocolchicoside-assisted AgNPs, Wound pathogens.

 DOI: http://dx.doi.org/10.22159/ajpcr.2026v19i4.58046. Journal homepage: https://innovareacademics.in/journals/index.php/ajpcr

INTRODUCTION

Biofilm-related contaminations pose a critical threat in medical care because of their upgraded protection from regular antimicrobial treatment [1]. *Pseudomonas aeruginosa* and *Enterococcus faecalis* are two conspicuous microbes known for their capacity to form vigorous biofilms, prompting determined infections and treatment disappointments. The audit highlighted the need for innovative strategies to disrupt *E. faecalis biofilms* and improve the success rates of endodontic treatments [2]. Nanotechnology facilitates molecular-scale manipulation of biomedical materials using engineered nanoparticles (1–100 nm), which possess unique physicochemical properties such as high surface-area-to-volume ratios, increased reactivity, and the ability to interact at the subcellular level [28]. Silver nanoparticles (AgNPs) have shown promise as effective agents against biofilm-related diseases due to their broad-spectrum antimicrobial activity and their ability to penetrate biofilm networks. AgNPs have shown promise as successful specialists against biofilm-related diseases because of their wide range of antimicrobial activity and capacity to enter biofilm networks [3,4]. Furthermore, the mix of AgNPs with different specialists has shown promise in upgrading their antimicrobial viability against different microorganisms, including *P. aeruginosa* and *E. faecalis* [5,6]. A study examined the components of the activity of AgNPs in upsetting biofilms, including layer damage, reactive oxygen species generation, and impedance with cellular processes [7]. The synergistic antimicrobial action of thiocolchicoside-mediated AgNPs (TC-AgNCs) enhances their effectiveness against a wide range of microbial pathogens [8]. Wound diseases present huge difficulties in clinical settings, frequently prompting delayed recovery times, expanded medical care costs, and elevated patient distress [23]. Resolving this issue requires powerful antimicrobial specialists to actually battle wound microbes. One promising methodology includes the usage of nanoparticles, especially AgNPs, because of their remarkable properties [29]. The antimicrobial movement of TC-AgNPs comes from their capacity to prompt oxidative pressure, disturb cell layers, and disrupt fundamental cellular processes in microorganisms [9]. Silver particles let out of TC-AgNPs are associated with sulfur-containing proteins and mixtures, prompting the restraint of key metabolic pathways. Besides, the high surface region-to-volume proportion of nanoparticles works with proficient cooperation with microbial surfaces, upgrading their antimicrobial viability against a great many microorganisms, including bacteria, parasites, and infections [10,24]. *In vitro* examinations have exhibited the adequacy of TC-AgNPs against normal injury microorganisms, for example, *S. aureus*, *P. aeruginosa*, and *Candida albicans*. TC-AgNPs highlight their true capacity as adjunctive specialists for contaminated wounds [11,12]. Furthermore, histopathological assessment of tissue

tests from animal models surveys the biocompatibility and tissue reactions following TC-AgNPs treatment [13]. Regardless of their genuine cutoff, several difficulties should be looked out for before the clinical interpretation of TC-AgNPs for wound healing [14,26]. These combine the progress of adaptable blend procedures, improvement of nanoparticle adequacy, clarification of extended length consequences for injury correcting, and examination of facilitated endeavors with safe cells [15]. In addition, administrative guaranteeing and normalization of TC-AgNP plans are fundamental to guarantee their security and adequacy in clinical practice [16,27].

METHODS

Chemicals required and instrument

Sigma-Aldrich Chemical Reagent Co., Ltd. supplied us with easily available food-grade thiocolchicoside (SRL catalog number 94066 and purity is 98%), silver nitrate ($AgNO_3$) (chemicals catalog number 71470SG025, purity is 99%), 1X phosphate-buffered saline (PBS) (HI Media, catalog number ML023, and the purity is 99.9%), LB medium (HI media, catalog number M1245 and purity is 94%), crystal violet (HI Media, catalog number SO12), amoxicillin, (Sigma-Aldrich, St. Louis, MO, USA; purity ≥98% Labmox concentration 10 mg/10ml) and (Muller Hinton Agar HI media catalog number M391 purity) used in this study were of analytical purity. The following instrument were used in the present study: orbital shaker (Lark), magnetic stirrer (Remi), double beam ultraviolet-visible (UV-vis) spectrophotometer-2377, microplate reader (Company name Agilent Model EPOCH2NSC), and TEM analysis (Thermo Fisher Scientific company model: Talos F 200i).

Preparation of *Gloriosa superba* plant extract

Freshly collected *G. superba* plant powder (0.5 g) was mixed with 50 mL of filtered water and heated at 50°C for 15–20 min. The mixture was then filtered through cotton fabric to obtain a clear plant extract, which was used for nanoparticle synthesis.

Synthesis of AgNPs

To 25 mL of *G. superba* plant extract, 2 mM $AgNO_3$ solution (0.034 g in 75 mL filtered water) was added. The mixture was stirred at 500 rpm for 24 h at room temperature. The resultant solution was centrifuged at 8000 rpm for 10 min. The supernatant was discarded, and the pellet containing AgNPs was collected and dried overnight at 60°C in a hot-air oven. The dried AgNPs were stored for further characterization and biological studies.

Preparation of thiocolchicoside-loaded AgNPs (TC-AgNPs)

After weighing 100 mg of thiocolchicoside, it was diluted in 1ml of distilled water, completely mixed, and kept properly for use later on [21]. Thiocolchicoside solution and AgNPs were mixed in a 1:1 ratio to obtain the thiocolchicoside-AgNP formulation, which was used for subsequent activity studies.

Antibiofilm activity

Antibiofilm activity was assessed using the crystal violet microtiter plate assay. Bacterial cultures isolated from colonies were grown overnight in Luria–Bertani (LB) broth and subsequently diluted with fresh medium, 200 µL of the bacterial suspension was dispensed into each well of a sterile 96-well microtiter plate and incubated at 37°C for 24 h to promote biofilm development. After incubation, free-floating cells were discarded by gently removing the supernatant, and the wells were washed 3 times with 200 µL of PBS to eliminate loosely attached cells. The test samples at the required concentrations were added to the wells and incubated for 30 min at 37°C under mild shaking conditions. After treatment, the wells were rinsed 3 times with sterile distilled water and fixed with methanol for 20 min. The plates were then washed again with distilled water, air-dried, and stained with 1% (w/v) crystal violet for 10 min. Excess stain was removed by washing 3 times with distilled water. Finally, 200 µL of 95% ethanol was added to each well to dissolve the retained crystal violet, and biofilm formation was quantified by recording the absorbance at 595 nm using a microplate reader [25].

Protein leakage analysis-(thiocolchicoside-loaded AgNPs) NCs

To estimate the amount of DNA. The culture was extracted the next day using centrifugation for 10 min at 5000 rpm. After being cleaned, the pellet was again suspended in a 10× buffer (pH 7.2). A bacterial cell density of 1×10^5 cells/mL was maintained. Following treatment with TC+AgNPs nanocomposite, various aliquots of cell suspensions were incubated for 3 and 5 h at room temperature. As a control, the bacterial culture without the thiocolchicoside-loaded AgNPs nanocomposite was used. As a standard, an antibiotic (such as amoxicillin) was employed. Following a 10-min centrifugation at 5000 rpm in an incubator, the luminescence of the supernatant was detected at 260 nm.

The inquiry into protein leakage employed the Bradford test. For 24–48 h, bacterial cells from *S. aureus, P. aeruginosa, Escherichia coli*, and *E. faecalis* were exposed to different concentrations of thiocolchicoside AgNP nanocomposites. The corresponding values were 25, 50, and 100 µg/ml. As a standard, an antibiotic (such as amoxicillin) was employed. After treatment, the bacterial culture was centrifuged for 10 min at 3000 rpm to separate the uppermost phase, which was subsequently retrieved. Each sample required 200 µL of supernatant, which was then transferred to 96-well enzyme-linked immunosorbent assay plates. These were incubated for 10 min in a dark setting with 50 µL of Bradford reagent added. At 595 nm, the optical density (OD) of the sample was determined [22].

Cytoplasmic analysis-(thiocolchicoside-loaded AgNPs) NCs

Cytoplasmic components, including DNA and protein, are liberated from bacterial cells when they are treated with nanoparticles. Therefore, we have attempted to assess in this work the cytoplasmic leakage of bacterial cells following treatment with thiocolchicoside+AgNPs nanocomposite. Microbial broth containing *E. faecalis, E. coli, Pseudomonas,* and *S. aureus* (10 mL) was cultivated in an incubator and left overnight [21].

Antimicrobial activity

The antibacterial movement of the thiocolchicoside-loaded AgNPs nanocomposite was evaluated using the agar well dispersion technique. MHA plates were ready, sanitized utilizing an autoclave for 15–20 min at 121°C. Post-sanitization, the suspension was then spread on the outer layer of clean Petri dishes and allowed to return to normal ambient temperature. The bacterial species, including *E. faecalis, E. coli, Pseudomonas,* and *S. aureus,* were spread equitably onto the plates utilizing sterile q-tips. 9 mm breadth wells were made in the agar utilizing polystyrene tips. Various fixations (25, 50, and 100 µg/mL) of TC-SNCs were loaded. An anti-infection (e.g., microbes amoxyrite) was utilized as per norms. Plates were hatched at 37°C for 24 h and for a total of 48 h for parasitic societies. The AMA was assessed by estimating the distance across the restraint zone encompassing the wells. The diameter of the zone of hindrance was calculated using a ruler and kept in millimetres, and the zone of restriction was identified [20].

Statistical analysis

Statistical analysis was executed, two-way analysis of variance ANOVA using Bonferroni *post hoc* test for all groups compared, statistical analysis test run in replicate using GraphPad Prism version 8.0 software. It was determined that a p=0.05 was statistically significant. All of the investigations have been performed in three independent experiments, and the findings are presented as mean±SE. Applying the spreadsheet program Microsoft Excel, find out the values of thiocolchicosidesilver nanocomposite produced from *G. superba.*

RESULTS

Visual observation

During the biosynthesis process, the aqueous extract of *G. superba* initially exhibited a light brown coloration. The extract was filtered to remove insoluble plant residues, resulting in a clear filtrate. An aqueous solution of $AgNO_3$ was prepared separately and mixed with the plant extract. Upon addition of the extract to the $AgNO_3$ solution, a gradual color change from light brown to dark brown was observed, indicating

the reduction of Ag^+ ions and the formation of AgNPs. Following centrifugation, the synthesized AgNPs were obtained as a greenish pellet at the bottom of the centrifuge tube, confirming successful nanoparticle formation. Subsequently, thiocolchicoside was added to the AgNP suspension, resulting in the formation of a thiocolchicoside–silver nanocomposite as the final product Fig. 1.

UV-vis absorption spectrum of thiocolchicoside-assisted silver nanocomposite (TC-AgNCs)

The UV-Vis spectroscopic investigation of the synthesized nanomaterial revealed a distinct absorption band in the ultraviolet region, with a strong absorption peak at 250–270 nm. This peak is ascribed to the nanoparticles' surface plasmon resonance, indicating that they were successfully formed. The spectra also showed a progressive reduction in absorbance beyond 300 nm, with no additional strong peaks reaching 700 nm, indicating good particle stability and minimum aggregation. The broad absorption profile shows that the nanoparticles have a homogeneous size distribution. Reduced absorbance at higher wavelengths indicates well-dispersed nanoparticles and demonstrates the creation of stable nanostructures. I recorded the ultraviolet reading using a double-beam UV-Vis spectrophotometer (Fig. 2).

Transmission electron microscopy (TEM) analysis

Fig. 3 shows the TEM micrographs showing well-dispersed, predominantly spherical AgNPs with particle sizes in the range of approximately 5–30 nm. The TEM micrograph verifies the successful formation of AgNPs exhibiting predominantly spherical shapes. The nanoparticles are visible as dark, electron-dense features dispersed over a lighter matrix, which is typical of metallic silver. The particle size distribution ranges from approximately 5–30 nm, with most particles measuring below 20 nm in diameter. The nanoparticles show a fairly homogeneous distribution with negligible aggregation, reflecting efficient stabilization during the synthesis procedure. A small number of larger particles were also detected, possibly resulting from particle merging during the growth process. The well-defined particle outlines and uniform image contrast indicate the crystalline nature of the synthesized AgNPs. The TEM image is observed by the Talos F 200i model instrument.

Antibiofilm activity

The antibiofilm activity of the tested compound against *E. faecalis* and *Pseudomonas* spp. was evaluated by measuring OD as an indicator of biofilm formation. The results showed a dose-dependent reduction in biofilm formation, with mean OD values (± standard error) of 0.525±0.015 and 0.54±0.015 at 25 µg/mL, decreasing to 0.455±0.005 and 0.46±0.005 at 100 µg/mL for *E. faecalis* and *Pseudomonas* spp., respectively. The standard treatment exhibited OD values of 0.42±0.0 for both strains, whereas the untreated control showed the highest biofilm formation with OD values of 0.555±0.005 and 0.56±0.005. These findings indicate that the compound effectively inhibits biofilm formation in both bacterial species in a concentration-dependent manner. Overall, the test chemical showed strong antibiofilm activity, especially at higher concentrations, as seen by lower OD values with little standard error, indicating good experimental repeatability (Fig. 4).

Protein leakage analysis

The protein leakage assay was performed to evaluate the effect of the tested compound on *E. faecalis* and *Pseudomonas* spp., using OD as an indicator of protein release. The results demonstrated a slight, concentration-dependent increase in protein leakage, with mean OD values (±standard error) of 0.34±0.006 and 0.36±0.006 at 25 µg/mL, rising to 0.38±0.006 and 0.39±0.006 at 100 µg/mL for *E. faecalis* and *Pseudomonas* spp., respectively. The standard treatment showed OD values of 0.39±0.006 and 0.41±0.006, whereas the untreated control exhibited the lowest protein leakage, with OD values of 0.32±0.006 and 0.35±0.006 for the two strains, respectively. These findings suggest that the compound induces protein leakage in both bacterial species, with slightly higher concentrations promoting more leakage. Overall, the test compound demonstrated a moderate effect on protein release, with low standard error values indicating consistent experimental reproducibility (Fig. 5).

Cytoplasmic analysis

The cytoplasmic leakage assay was conducted to evaluate the effect of thiocolchicoside combined with silver nanocomposite (NCs) on *Pseudomonas* spp. *and E. faecalis*, using OD as an indicator of protein release. The results showed a concentration-dependent increase in protein leakage, with mean OD values (±standard error) of 0.31±0.01 and 0.28±0.01 at 25 µg/mL, rising to 0.38±0.01 and 0.31±0.01 at 100 µg/mL for *Pseudomonas* spp. and *E. faecalis*, respectively. The standard treatment exhibited OD values of 0.39±0.01 and 0.33±0.01, whereas the untreated control showed the lowest protein leakage, with OD values of 0.30±0.01 and 0.26±0.01 for the two strains, respectively. These findings indicate that the tested NCs induce cytoplasmic protein leakage in both bacterial species, with higher concentrations causing slightly more leakage. Overall, the compound demonstrates moderate cytoplasmic disruption with low standard error values, indicating consistent experimental reproducibility (Fig. 6).

Antimicrobial activity

Fig. 7 illustrates the antimicrobial activity of thiocolchicoside-loaded silver nanocomposite (TC-AgNCs) against *E. faecalis, E. coli, Pseudomonas* spp., and *S. aureus* at varying concentrations. A clear concentration-dependent increase in the zone of inhibition is observed for all tested pathogens, with maximum activity at 100 µg/mL. Among the organisms, *Pseudomonas* spp. exhibited the highest susceptibility, followed by *E. faecalis* and *S. aureus*. In contrast, the control group showed minimal inhibitory effect, confirming the antimicrobial role of TC-AgNCs. These results demonstrate the broad-spectrum antibacterial potential of TC-AgNCs against both Gram-positive and Gram-negative bacteria. Table 1 expresses the progressively increasing regions of inhibition from 25 to 100 µg/mL, demonstrating the nanocomposite's dose-dependent increase in antibacterial activity against all tested pathogens. The most susceptible bacteria were *Pseudomonas* spp., *E. coli, S. aureus*, and *E. faecalis*. Good experimental repeatability is indicated by the continuously low standard error values. The control group, on the other hand, showed very few zones of inhibition, indicating that there was no antibacterial activity in the absence of therapy.

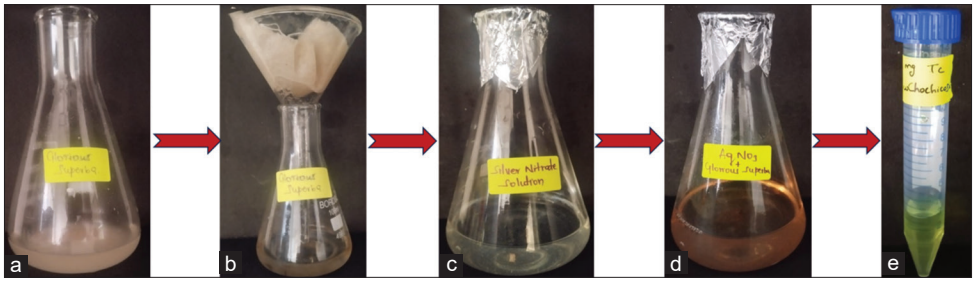

Fig. 1: Green synthesis of silver nanoparticles mediated by thiocolchicoside nanocomposite (a) *Gloriosa superba*, (b) filtration of the plant extract, (c) prepared aqueous silver nitrate ($AgNO_3$) solution before reaction, (d) *G. superba* extract with $AgNO_3$, (e) thiocolchicoside

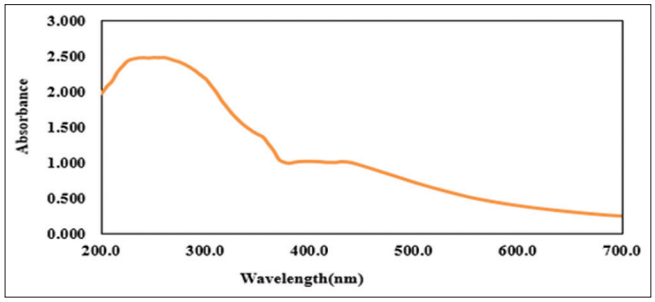

Fig. 2: Ultraviolet-visible spectroscopic analysis of thiocolchicoside-assisted silver nanocomposite

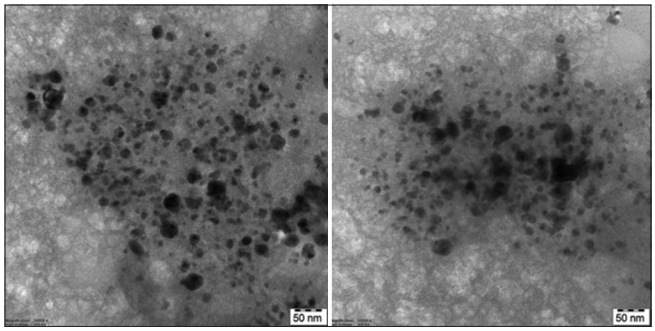

Fig. 3: Transmission electron microscopy analysis of thiocolchicoside-assisted silver nanocomposite

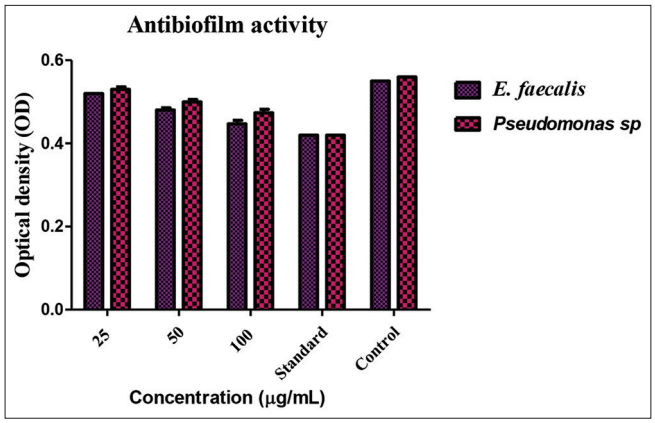

Fig. 4. Antibiofilm activity of Thiocolchicoside-loaded silver nanocomposite against E. faecalis and Pseudomonas sp. at different concentrations, showing reduced biofilm mass compared to the control. The Two-way repeated measures ANOVA showed a significant value of (p = 0.0439, *), a highly significant effect.

Time kill curve assay of thiocolchicoside-loaded AgNPs (TC-AgNCs)

Fig. 8 depicts the time-dependent antibacterial action of thiocolchicoside-functionalized silver nanocomposite (Ag NCs) against *E. faecalis*, *E. coli*, *Pseudomonas* spp., and *S. aureus*. A progressive decline in bacterial counts (log colony-forming unit/mL) was noted with increasing nanoparticle concentration and incubation time. The 100 µg/mL dose showed the strongest inhibitory effect, comparable to the standard. Lower doses produced consistent but moderate suppression. Overall, the findings confirm a dose- and time-dependent antibacterial activity of thiocolchicoside-AgNPs against both Gram-positive and Gram-negative strains.

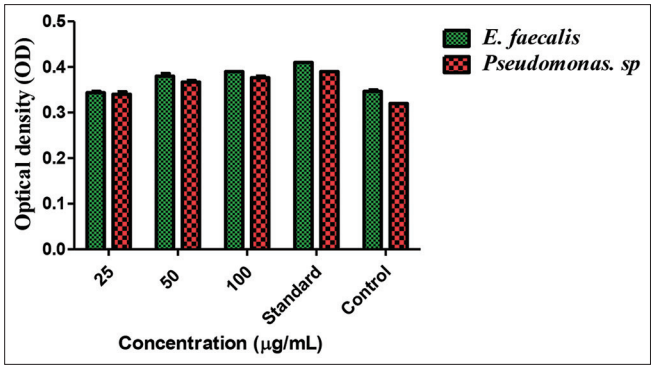

Fig. 5: Protein leakage analysis of Thiocolchicoside + Ag nanocomposites against Pseudomonas sp. and E. faecalis at varying concentrations compared with standard and control groups. The Two-way repeated measures ANOVA revealed a significant value (p = 0.0195, *), a highly significant effect

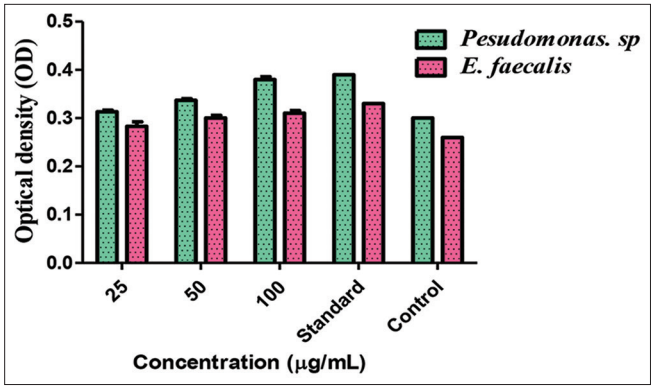

Fig. 6: Cytoplasmic leakage analysis of Thiocolchicoside + silver nanocomposites against Pseudomonas sp. and E. faecalis at different concentrations compared with standard and control groups. Two-way repeated measures ANOVA showed significant value (p = 0.0017 **)

DISCUSSION

The rise of biofilm-related diseases represents a huge challenge in medical care settings, requiring the improvement of powerful remedial techniques. In this review, we explored the counter-biofilm movement of thiocolchicoside-interceded silver nanoparticles (TC-SNPs) against two clinically applicable microbes, *P. aeruginosa* and *E. faecalis.* Our discoveries show that TC-SNPs display an intense enemy of biofilm action against both *P. aeruginosa* and *E. faecalis*. This perception is upheld by the huge decrease in biofilm arrangement following TC-SNPs treatment, as proven by gem violet staining and confocal laser scanning microscopy. The disturbance of biofilm design, described by decreases in thickness and biomass, features the adequacy of TC-SNPs in hindering biofilm advancement [13]. Moreover, our review uncovered that TC-SNPs prompt protein spillage from biofilm-encased bacterial cells, demonstrating the disturbance of cell layer integrity. This peculiarity was especially evident in both *P. aeruginosa and E. faecalis* biofilms treated with TC-SNPs, proposing a system by which TC-SNPs apply their enemy of biofilm impact [14]. The arrival of genomic material, as shown by DNA spillage measures, further backs the idea of TC-SNPs disturbing nucleic corrosive trustworthiness inside biofilm-installed bacterial cells [16]. Furthermore, explaining the exact instruments fundamental to the counter biofilm action of TC-SNPs, incorporating their communications with bacterial cells and biofilm network parts, requires thorough atomic investigations [17]. Antimicrobial activities against wound pathogens such as *E. faecalis,*

Table 1: Zone of inhibition (mm) – Mean±SE of thiocolchicoside-assisted silver nanocomposite

Concentration (µg/mL)	*Enterococcus faecalis*	*Escherichia coli*	*Pseudomonas* spp.	*Staphylococcus aureus*
25	16.0±0.8	14.0±0.7	20.0±0.9	14.5±0.7
50	17.5±0.8	15.0±0.7	21.5±0.9	16.0±0.8
100	18.5±0.9	16.0±0.8	22.5±1.0	18.0±0.9
Control	9.0±0.5	8.5±0.5	9.0±0.5	9.0±0.5

SE: Standard error

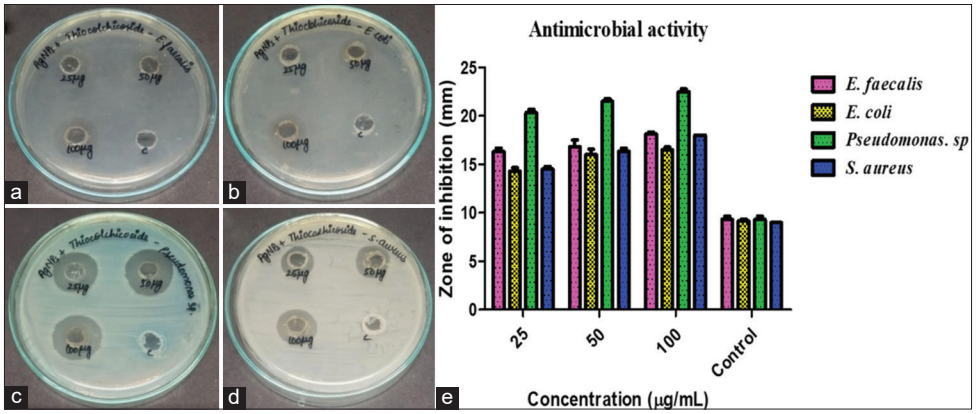

Fig. 7: Antimicrobial activity of Thiocolchicoside-assisted silver nanocomposite (TC-AgNCs) showing zone of inhibition against E. faecalis, E. coli, Pseudomonas sp., and S. aureus at different concentrations. Two-way repeated measures ANOVA showed a significant value (p < 0.0001, *)**

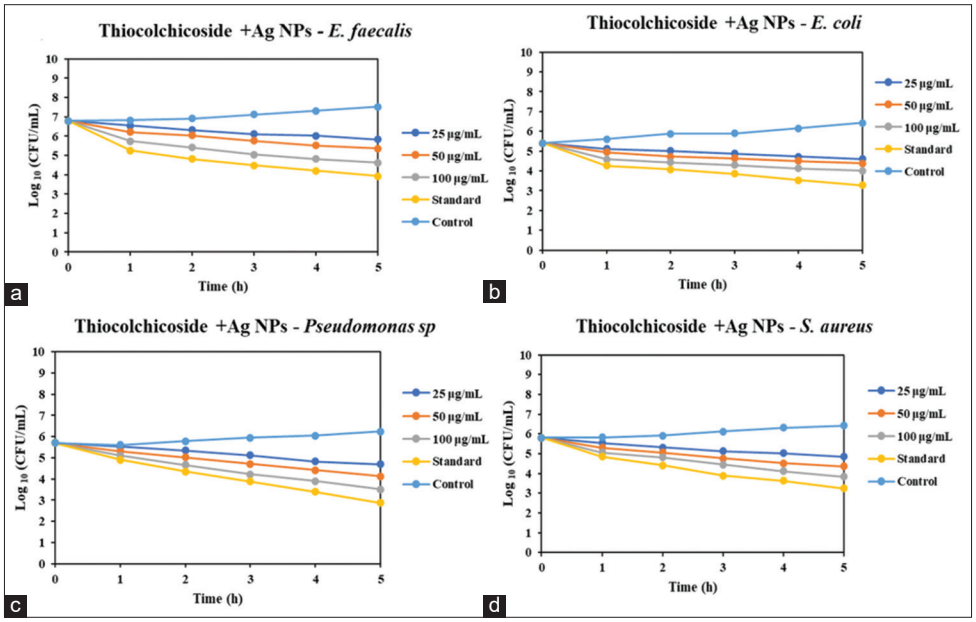

Fig. 8: Time-dependent antibacterial activity of Thiocolchicoside-loaded silver nanocomposite (Ag NCs) against E. faecalis, E. coli, Pseudomonas sp., and S. aureus at different concentrations. Time-kill curve analysis revealed a significant effect of time on bacterial counts for all tested species (p < 0.0001, *). Higher concentrations of Thiocolchicoside + Ag NCs also showed a significant effect**

E. coli, Pseudomonas, and *S. aureus.* The antibacterial effect of green integrated TC-SNPs was evaluated using the agar well dispersion approach, a deep-rooted procedure for surveying the viability of antimicrobial specialists [18]. The strategy included planning Mueller Hinton agar plates and immunizing them with bacterial and contagious suspensions, including *Streptococcus mutans, Lactobacillus* spp., *S. aureus,* and *C. albicans* [19].

CONCLUSION

All in all, our review gives undeniable proof of the adequacy of thiocolchicoside-intervened AgNPs (TC-SNPs) as powerful specialists against biofilm-related diseases brought about by *P. aeruginosa* and *E. faecalis*. Through complete *in vitro* appraisals, we showed that TC-SNPs really hinder biofilm formation and disturb pre-formed biofilms of these clinically important microorganisms. The critical decrease in biofilm biomass and design following TC-SNPs treatment highlights their true capacity as promising restorative specialists. Furthermore, the noticed protein spillage and DNA spillage from biofilm-encased bacterial cells propose instruments by which TC-SNPs apply their enemy of biofilm action, including interruption of cell film integrity and nucleic acid stability.

Overall, the agar well dispersion approach was used to assess the antibacterial effect of green-orchestrated TC-SNPs toward a range of harmful microorganisms, particularly germs and parasites. By getting Mueller Hinton agar plates and inoculating them with bacterial and contagious suspensions, the review guaranteed normalized conditions for surveying the adequacy of TC-SNPs across different microorganisms. The outcomes obtained from the investigation, including the estimation of restraint zone distances across encompassing wells containing various groupings of TC-SNPs, gave quantitative information on the antimicrobial power of these nanoparticles. The noticed hindrance zones act as signs of TC-SNPs' capacity to obstruct the development of pathogenic microorganisms, featuring their true capacity as antimicrobial specialists.

FUNDING

This study did not receive any specific grant from funding agencies in the public, commercial, or not-for-profit sectors.

ETHICS APPROVAL AND CONSENT TO PARTICIPATE

All the data were available from public databases, and there is no need for ethics approval and consent.

CREDIT AUTHORSHIP CONTRIBUTION STATEMENT

PP: Writing-Review and editing, writing. VR: Original draft, methodology, RKS: Data curation, visualization, drew the figures and pictures. DN: Helped in writing the manuscript and revised it. SJ: Validation and editing with review of the manuscript. RS: Designed protocols for all the experiments, supervised, proofread, analyzed the data, and revised the reviewer's comments, investigation, and conceptualization. All authors reviewed and discussed the results, provided comments on the manuscript, and approved its final published version.

CONSENT FOR PUBLICATION

Not applicable.

CONFLICT OF INTEREST

The authors state no conflict of interest

DECLARATION OF COMPETING INTEREST

The authors declare that they have no conflict of interest.

REFERENCES

1. Khan MA, Celik I, Khan HM, Shahid M, Shahzad A, Kumar S. Antibiofilm and anti-quorum sensing activity of *Psidium guajava* L. Leaf extract: *In vitro* and *in silico* approach. PLOS One. 2023;18(12):e0295524. doi: 10.1371/journal.pone.0295524, PMID 38113217
2. Paganelli FL, Van De Kamer T, Brouwer EC, Leavis HL, Woodford N, Bonten MJ. Lipoteichoic acid synthesis inhibition in combination with antibiotics abrogates growth of multidrug-resistant *Enterococcus faecium*. Int J Antimicrob Agents. 2017;49(3):355-63. doi: 10.1016/j.ijantimicag.2016.12.002, PMID 28188831
3. Chatterjee AK, Sarkar RK, Chattopadhyay AP, Aich P, Chakraborty R, Basu T. A simple robust method for synthesis of metallic copper nanoparticles of high antibacterial potency against *E. coli*. Nanotechnology. 2012;23(8):085103. doi: 10.1088/0957-4484/23/8/085103, PMID 22293320
4. Ruparelia JP, Chatterjee AK, Duttagupta SP, Mukherji S. Strain specificity in antimicrobial activity of silver and copper nanoparticles. Acta Biomater. 2008;4(3):707-16. doi: 10.1016/j.actbio.2007.11.006, PMID 18248860
5. Gunalan S, Sivaraj R, Venckatesh R. *Aloe barbadensis* Miller mediated green synthesis of mono-disperse copper oxide nanoparticles: Optical properties. Spectrochim Acta A Mol Biomol Spectrosc. 2012;97:1140-4. doi: 10.1016/j.saa.2012.07.096, PMID 22940049
6. Martinez-Gutierrez F, Olive PL, Banuelos A, Orrantia E, Nino N, Sanchez EM. Synthesis, characterization, and evaluation of antimicrobial and cytotoxic effect of silver and titanium nanoparticles. Nanomedicine. 2010;6(5):681-8. doi: 10.1016/j.nano.2010.02.001, PMID 20215045
7. Durán N, Durán M, De Jesus MB, Seabra AB, Fávaro WJ, Nakazato G. Silver nanoparticles: A new view on mechanistic aspects on antimicrobial activity. Nanomedicine. 2016;12(3):789-99. doi: 10.1016/j.nano.2015.11.016, PMID 26724539
8. Sasarom M, Wanachantararak P, Chaijareenont P, Okonogi S. Biosynthesis of copper oxide nanoparticles using *Caesalpinia sappan* extract: *In vitro* evaluation of antifungal and antibiofilm activities against *Candida albicans*. Drug Discov Ther. 2023;17(4):238-47. doi: 10.5582/ddt.2023.01032, PMID 37612046
9. Pollini M, Paladini F. The emerging role of silk fibroin for the development of novel drug delivery systems. Biomimetics (Basel). 2024;9(5):295. doi: 10.3390/biomimetics9050295, PMID 38786505
10. Gunasekaran T, Haile T, Nigusse T, Dhanaraju MD. Nanotechnology: An effective tool for enhancing bioavailability and bioactivity of phytomedicine. Asian Pac J Trop Biomed. 2014;4(Suppl 1):S1-7. doi: 10.12980/apjtb.4.2014c980, PMID 25183064
11. Rai M, Ingle AP, Birla S, Yadav A, Santos CA. Strategic role of selected noble metal nanoparticles in medicine. Crit Rev Microbiol. 2016;42(5):696-719. doi: 10.3109/1040841X.2015.1018131, PMID 26089024
12. Shanmugam, R., Munusamy, T., Jayakodi, S., Al-Ghanim, K. A., Nicoletti, M., Sachivkina, N., & Govindarajan, M. (2023). Probiotic-bacteria (Lactobacillus fermentum)-wrapped zinc oxide nanoparticles: biosynthesis, characterization, and antibacterial activity. Fermentation, 9(5), 413.
13. Yang J, Zhang L, He X, Gou X, Zong Z, Luo Y. *In vitro* and *in vivo* enhancement effect of glabridin on the antibacterial activity of colistin, against multidrug resistant *Escherichia coli* strains. Phytomedicine. 2024;130:155732. doi: 10.1016/j.phymed.2024.155732, PMID 38776738
14. Arasu MV, Al-Dhabi NA. Antibacterial activity of peptides and bio-safety evaluation: *In vitro* and *in vivo* studies against bacterial and fungal pathogens. J Infect Public Health. 2023;16(12):2031-7. doi: 10.1016/j.jiph.2023.09.006, PMID 37890227
15. Pelgrift RY, Friedman AJ. Nanotechnology as a therapeutic tool to combat microbial resistance. Adv Drug Deliv Rev. 2013;65(13-14):1803-15. doi: 10.1016/j.addr.2013.07.011, PMID 23892192
16. Tan X, Huang Y, Rana A, Singh N, Abbey TC, Chen H. Optimization of an *in vitro Pseudomonas aeruginosa* biofilm model to examine antibiotic pharmacodynamics at the air-liquid interface. NPJ Biofilms Microbiomes. 2024;10(1):16. doi: 10.1038/s41522-024-00483-y, PMID 38429317
17. Jayakumar J, Vinod V, Arumugam T, Sathy BN, Biswas L, Kumar VA. Efficacy of lysostaphin functionalized silicon catheter for the prevention of *Staphylococcus aureus* biofilm. Int J Biol Macromol. 2024;256(2):128547. doi: 10.1016/j.ijbiomac.2023.128547, PMID 38048926
18. Lin H, Zhou R, Zhang M, Huang R, Fan C, Zhou S. *In vitro* antibacterial activity of a novel acid-activated antimicrobial peptide against *Streptococcus mutans*. Curr Protein Pept Sci. 2024;25(1):83-93. doi: 10.2174/1389203724666230818111515, PMID 37594108
19. Wen Z, Chen C, Shang Y, Fan K, Li P, Li C. Baohuoside I inhibits virulence of multidrug-resistant *Staphylococcus aureus* by targeting the transcription *Staphylococcus* accessory regulator factor SarZ. Phytomedicine. 2024;130:155590. doi: 10.1016/j.phymed.2024.155590, PMID 38810547
20. Anishya D, Jain RK. Vanillin-mediated green-synthesised silver nanoparticles' characterisation and antimicrobial activity: An *in-vitro* study. Cureus. 2024;16(1):e51659. doi: 10.7759/cureus.51659, PMID 38318582
21. Sahoo, B., Panigrahi, L. L., Jena, S., Jha, S., & Arakha, M. (2023). Oxidative stress generated due to photocatalytic activity of biosynthesized selenium nanoparticles triggers cytoplasmic leakage leading to bacterial cell death. RSC advances, 13(17), 11406-11414.
22. Azeem M, Siddique MH, Imran M, Zubair M, Mumtaz R, Younas M, Abdel-Maksoud MA. Assessing anticancer, antidiabetic, and antioxidant capacities in green-synthesized zinc oxide nanoparticles and solvent-based plant extracts. Heliyon. 2024;10(14):e34073.
23. Ahmajärvi, K. M., Isoherranen, K. M., Pessi, T. J., & Venermo, M. A. (2025). The Impact of Diagnostic Delay on Wound Healing—A Cohort Study in a Primary Care Setting. International wound journal, 22(5), e70141.
24. Pauline CR, Akshita TP, Kannan K, Sivaperumal P. Characterization and biological activity of silver nanoparticles from (Rhizophora mucronata) Mangrove extract. Nano Life. 2025;15(3):2450018.

25. Jabeen N, Prabhalakshmi K, Dhanraj G, Ramasubburayan R. Biosynthesis of titanium dioxide nanoparticles using *Sargassum tenerrimum* as reductant and deciphering its antibiofilm role against cariogenic *Candida albicans*. Microb Pathog. 2025;202:107452. doi: 10.1016/j.micpath.2025.107452, PMID 40057005
26. Le NT, Thi TT, Ching YC, Nguyen NH, Nguyen DY, Truong QM. *Garcinia mangostana* shell and *Tradescantia spathacea* leaf extract-mediated one-pot synthesis of silver nanoparticles with effective antifungal properties. Curr Nanosci. 2021;17(5):762-71. doi: 10.2174/1573413716666201222111244
27. Asha S, Asha A, Rajeshkumar S. Evaluation of phytochemical constituents and antimicrobial activity of silver nanoparticle synthesized *Ipomoea nil* against selected pathogens. Asian J Pharm Clin Res. 2017:183-7.
28. Nadeesh T, Dhara S, Manna P, Kayal P. Advanced nanotherapeutics in multiple sclerosis treatment: From blood-brain barrier crossing to remyelination enhancement. Int J Appl Pharm. 2026;18(1):71-83.
29. Manibhushanam S, Srinivasan UM, Narayanasamy D. Nanoparticle-embedded microneedles for enhanced transdermal delivery: Advances and applications. Int J Appl Pharm. 2026;18(1):20-32. doi: 10.22159/ijap.2026v18i1.55869